NASA Technical Memorandum 110387

Recent Developments in Gun Operating Techniques at the NASA Ames Ballistic Ranges

D. W. Bogdanoff, Thermosciences Institute, Ames Research Center, Moffett Field, California
R. J. Miller, Ames Research Center, Moffett Field, California

March 1996

National Aeronautics and
Space Administration

Ames Research Center
Moffett Field, California 94035-1000

Recent Developments in Gun Operating Techniques at the NASA Ames Ballistic Ranges

D. W. BOGDANOFF*

Thermosciences Institute

Ames Research Center

and

R. J. MILLER†

Ames Research Center

Summary

This paper describes recent developments in gun operating techniques at the Ames ballistic range complex. This range complex has been in operation since the early 1960s. Behavior of sabots during separation and projectile-target impact phenomena have long been observed by means of short-duration flash X-rays: new versions allow operation in the lower-energy ("soft") X-ray range and have been found to be more effective than the earlier designs. The dynamics of sabot separation is investigated in some depth from X-ray photographs of sabots launched in the Ames 1.0" and 1.5" guns; the sabot separation dynamics appears to be in reasonably good agreement with standard aerodynamic theory. Certain sabot packages appear to suffer no erosion or plastic deformation on traversing the gun barrel, contrary to what would be expected. Gun erosion data from the Ames 0.5", 1.0", and 1.5" guns is examined in detail and can be correlated with a particular non-dimensionalized powder mass parameter. The gun erosion increases very rapidly as this parameter is increased. Representative shapes of eroded gun barrels are given. Guided by a computational fluid dynamics (CFD) code, the operating conditions of the Ames 0.5" and 1.5" guns were modified. These changes involved (1) reduction in the piston mass, powder mass and hydrogen fill pressure and (2) reduction in pump tube volume, while maintaining hydrogen mass. These changes resulted in muzzle velocity increases of 0.5–0.8 km/sec, achieved simultaneously with 30–50 percent reductions in gun erosion.

*Senior Research Scientist.
†Branch Scientist (retired).

I. Introduction

Ballistic ranges (ref. 1) provide much valuable information on hypersonic aerodynamics and vehicle stability, radiation from the gas surrounding vehicles in hypersonic flight, impact of space debris on space vehicles and in number of other areas. The Hypervelocity Free Flight (HFF) facility at NASA's Ames Research Center is a ballistic range complex that was built in 1963–64. Development of launch guns and techniques was carried on extensively until about 1969, but budget and schedule pressures essentially froze technology at that state until 1993. However, over the time period 1993–96, there has been considerable activity in the Ames ballistic range complex. A number of techniques for improving the quality of range data, obtaining more reliable, consistent launches, improving gun component life, and improving gun performance have been developed and are reported here.

The traditional "hard" X-ray techniques (ref. 2) frequently result in rather poor definition of the projectile. New X-ray techniques (using "soft" X-rays) will be shown to yield improved resolution. Traditional sabot designs (ref. 3) usually have a cylindrical outer surface which rides on the bore of the barrel. A new design, presented here, with three lands on the outer surface, is also shown to produce consistent separations and a high percentage of successful launches. X-ray examination of the separation of these sabots suggests that the behavior of the sabots in flight can be fairly well explained by the traditional aerodynamic theory. However, the elastic energy may be important in the initial separation of the sabot on exiting the barrel, and the behavior of the sabot in the barrel seems, in some cases, to be completely elastic, showing no evidence of wear against the barrel walls.

Selecting gun operating conditions to minimize erosion (ref. 4) is a very important consideration for the launchers

in ballistic ranges. Reducing gun erosion can significantly increase the productivity of ballistic ranges (by reducing the down-time needed to replace barrels) and can increase the percentage of good launches obtained. Only very limited gun erosion data is available in the literature. A detailed study of gun erosion data for the NASA Ames 0.5", 1.0", and 1.5" guns is presented here. This study provides guidance on the selection of gun operating conditions to limit gun erosion and demonstrates that reduced gun erosion can be obtained upon reducing the pump tube length (while maintaining the hydrogen mass in the pump tube). The very detrimental effect of having helium in the pump tube is also shown. Representative shapes of eroded launch tubes for the Ames 0.5" and 1.5" guns are presented.

Support for DWB by NASA (Contract NAS-2-14031) to Eloret is gratefully acknowledged.

II. Soft X-rays

In common with most ballistic facilities, Ames uses flash X-rays for information on sabot/model separation and impact phenomena. In early operations, two 105 kV channels with a 70 nsec pulse duration were used. In recent operations, two 150 kV/70 nsec channels were added. One of the 105 kV channels has since failed. The original units were manufactured by the Field Emission Corporation, currently under Hewlett-Packard corporate ownership.

In the case of the recently acquired 150 kV channels, a so-called "soft" or low energy option was available, obtained by substituting a flash tube with a beryllium window at the front for the usual X-ray flash tube. In this case, the spectrum of X-rays emitted at the internal source is the same, but the low-energy tail, which has relatively low penetrating ability in most materials, is attenuated much less by the beryllium and is available to expose the film.

The usual film cassettes (for use with a hard X-ray system) have a hard face (usually a phenolic plastic material) and image-intensifying phosphor screens on both faces of the double-coated film. The film cassettes for use with soft X-rays are somewhat different: there is a minimal protective layer and there is no intensifying screen on the source side. In the present instance, a package of corrugated cardboard to provide a small amount of protection against blast and fragments, with an outer wrap of black polyethylene for light exclusion was devised, and a phosphor screen was used on the side away from the source. A 1.2-cm layer of foam was placed over the package for additional protection when used at the target.

Figure 1 shows X-rays of the beginning of sabot separation around a 1.27 cm aluminum sphere fired from the Ames 1.5" gun at 6.6 km/sec. The sabot was made of Lexan. Both hard and soft X-ray photographs are shown. They were taken simultaneously by stacking a soft X-ray film cassette as described above directly on top of a standard hard X-ray cassette Note that the edges are significantly better defined with the soft X-ray photograph. Since attenuation of X-rays is proportional to the mass of material in the path of the beam, where the object, in this case the sabot, tapers to a thin edge, the contrast at the edge falls to a very small value. The higher attenuation ratio of the soft X-rays produces greater contrast in these regions.

For the same reason, the soft X-ray technique allows imaging of smaller particles. This is illustrated in figure 2. The figure shows the debris cloud caused by the impact of a 1.27 cm diameter sphere at 6.59 km/sec on a 0.1905 cm thick aluminum plate at an angle of 55 deg from normal to the flightpath. Figure 3 is an older, hard X-ray picture. It shows sabot separation from an 0.95 cm sphere fired from the Ames 1.0" gun. The sabot that appears to have suffered a failure of the aerodynamic separation lip on one or more quarters, but the hard X-rays produce such low contrast in imaging the relatively thin material flying ahead that it is very difficult to draw useful conclusions. It is thought that the new soft X-ray system would have been much more effective in this case.

There is a separate problem of lack of sharpness that also degrades images. The source of the X-rays is an anode 2.5 mm in diameter. Since there is no feasible way to focus X-rays, simple ray-tracing shows that if the source-to-object distance is equal to the object-to-film distance, we may anticipate a penumbra 2.5 mm wide at each edge of the image. The actual size of the penumbra appears to be somewhat less, suggesting that the entire anode is not acting as a source. This effect is an inherent problem with X-rays that is essentially solvable only by moving the film quite close to the object. This, of course, carries the attendant risk of destroying the film by blast or fragments.

The higher-energy portion of the X-ray spectrum remains useful for imaging within larger masses of material. Figure 4 illustrates the formation of a crater by the impact of a 0.476 cm magnesium sphere at 6.6 km/sec on a thermal protection system tile. The LI-2200 tile is made of low density sintered ceramic, and is approximately 15 cm thick in the direction of X-ray penetration. This image was taken with an early 105 kV system and a hard X-ray film cassette. It shows an inner layer to the cavity, analogous to a shock front, that includes the projectile and

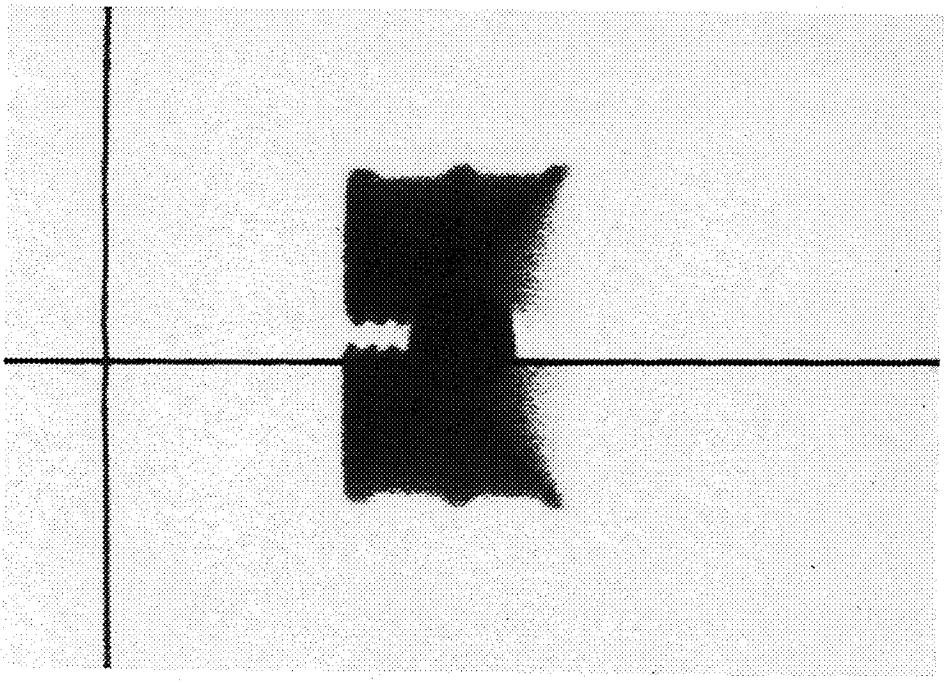

(a)

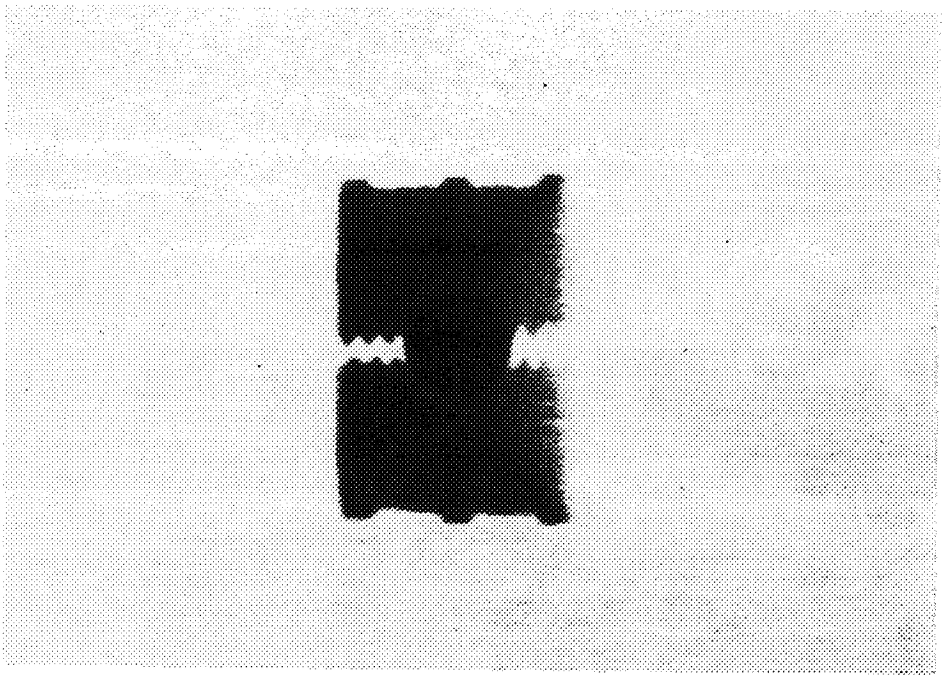

(b)

Figure 1. Beginning of separation of sabot around a 1.27 Al sphere fired from the Ames 1.5" gun at 6.6 km/sec. (a) Hard X-ray photograph, (b) soft X-ray photograph.

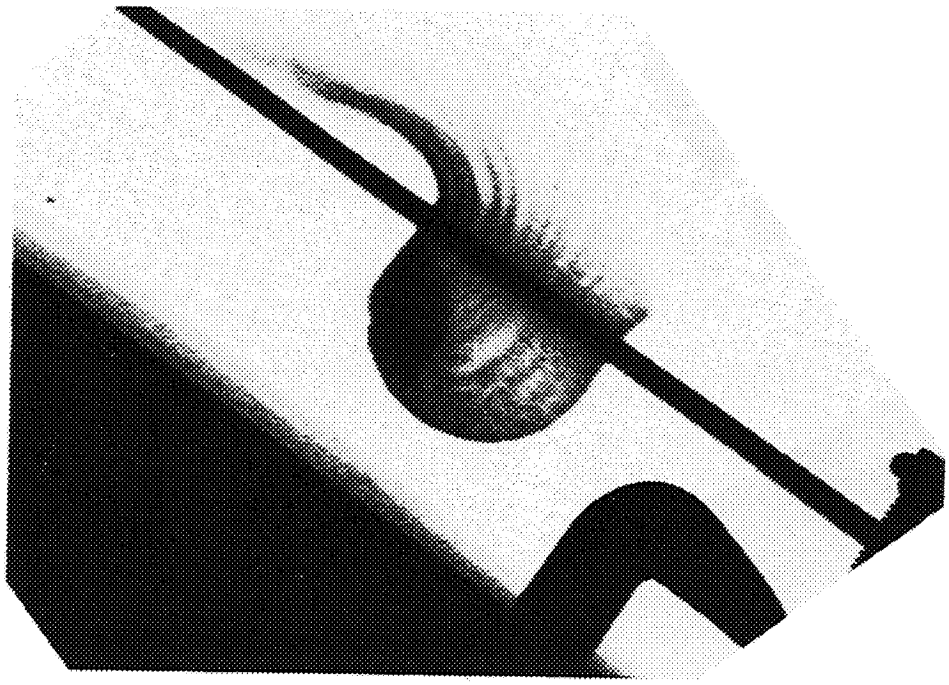

Figure 2. Soft X-ray photo of debris cloud produced by the impact of a 1.27 cm diameter sphere at 6.59 km/sec on a 0.1905 cm thick aluminum plate at an angle of 55 deg from normal to the flightpath.

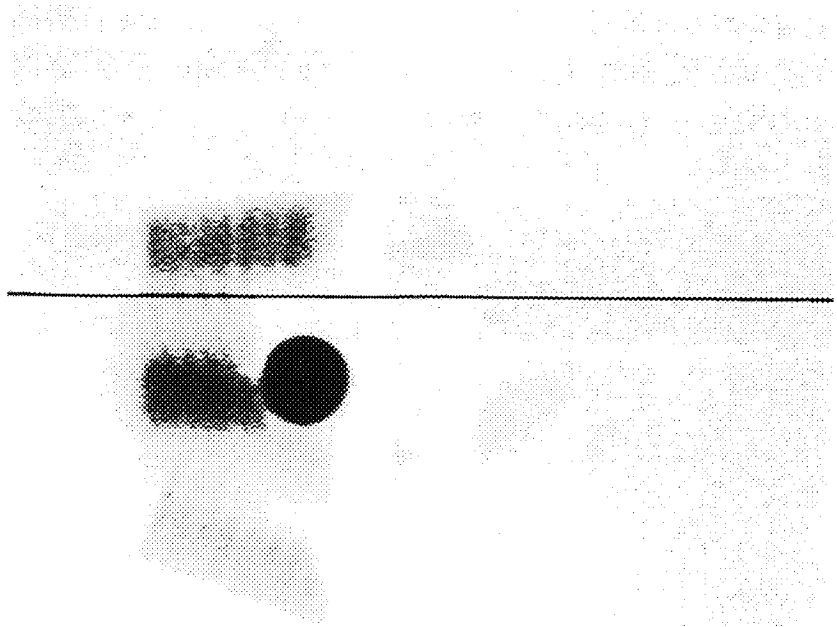

Figure 3. Hard X-ray picture of the sabot separation from a 0.95 cm aluminum sphere fired from the Ames 1.0" gun.

Figure 4. Hard X-ray picture of the formation of a crater by the impact of a 0.476 cm magnesium sphere at 6.6 km/sec on a thermal protection system tile.

material collected from the cavity already formed. This was taken approximately 37 μsec after first contact with the front face. This first contact was sensed by the closure of an electrical circuit between two layers of 13 micron thick Mylar mounted on the tile surface, each layer aluminized on one side and oriented so that the aluminized sides faced the approaching projectile. Further details of the impact tests of the thermal protection system tile are available in reference 5.

III. Sabot Design and Separation

Sabot design at Ames HFF facilities is constrained by the necessity of separating the sabot from the model by aerodynamic means, as none of the guns is rifled for spin separation. Sabots commonly have a conical-concave front face, and the separation process is envisioned to involve the dynamic pressure within the cavity applying an impulse to the two or four segments. Since this impulse is applied ahead of the center of gravity, it was expected to impart a rotational momentum about the base that would then expose the mating faces of the sabot to the dynamic pressure, which would in turn initiate the translational separation of the segments. Segments would accelerate away from the model at approximately constant rate, producing a parabolic flightpath. The quarters were expected to continue rotating as they diverge toward the conical steel stripper, 5.0 meters from the muzzle. The stripper has a central hole which allows free passage of the model, while intercepting and deflecting the sabot segments, preventing them from entering the instrumented test range.

Table 1 shows sabot separation data for a number of shots in the NASA Ames ballistic ranges. The first series of six shots was made using the Ames 1.0" gun in the HFF facility Aerodynamics range. Sabot observations were taken at two X-ray stations, 1.12 and 2.034 m from the muzzle. The sabot separation characteristics were defined by three parameters. First is the total sabot opening angle, measured between two opposite outside sabot surfaces (which ride on the gun barrel wall). Second is the mean (line) angle of these same two surfaces. A perfect sabot opening would always have zero angle here. A finite value here means that, on the average, the outside sabot surfaces are tilted either above or below the flight line; that is, the sabot as a whole has rotated about the flight line. These values given are absolute values only; the sign has been dropped. The third parameter is the sabot separation observed at the distance from the muzzle in question. The second series of seven shots was made using the Ames 1.5" gun in the HFF facility Radiation range. Sabot observations were taken at only one X-ray station, 0.81 m from the muzzle. For a larger number of shots for which shots R608-R617 are representative, sabot separation data was

Table 1. Sabot separation data from the NASA Ames 1.0" and 1.5" guns

Shot no.	Gun	Projectile diameter, mm	Air pressure in sabot separation region, Torr	Distance from muzzle, m	Total sabot opening angle, deg	Mean line angle of sabot, deg	Sabot separation, mm	Distance from muzzle, m	Total sabot opening angle, deg	Mean line angle of sabot, deg	Sabot separation, mm
A1869	1.0"	9.5	37.5	1.12	–0.7	2.1	8.1				
A1874	1.0"	9.5	45	1.12	–4	3	5.9				
A1889	1.0"	9.5	36	1.12	7	0.5	10.1	2.034	25.7	6.85	18.1
A1906	1.0"	12.7	35	1.12	1.4	4.5	6.8	2.034	8.8	9.1	21.7
A1907	1.0"	12.7	35	1.12	8.8	3.9	8.6	2.034	59.2/23.4	0.6/3.6	21.8
A190?	1.0"	12.7	35	1.12	7	3.5	6.6	2.034	41.8	0.9	14.8
Average	1.0"			1.12	3.3 (+5.5,–7.3)	2.9	7.7 (+2.4,–1.8)		29.4 (+29.8,–20.6)	5.6	19.1 (+2.7,–4.3)
R608	1.5"	12.7	32.8	0.81	2.7	2.9	2.4	5.05			76.4–90.4
R609	1.5"	12.7	34.1	0.81	2.5	0.2	2.9	(Note that this data for the 1.5" gun is not for the specific shots			
R610	1.5"	12.7	29.6	0.81	2.4	0.8	2	listed, but for a larger number of shots of which shots R608–R617			
R612	1.5"	12.7	28.4	0.81	–0.5	1.4	2.3	are representative. It is obtained from examining sabot strikes on the			
R613	1.5"	12.7	27.4	0.81	5	1.5	2.9	steel stripper cone. This data was taken from 5 stripper cones, each			
R615	1.5"	12.7	27.5	0.81	0	0	No data	bearing the strikes from 2 or more shots.)			
R617	1.5"	12.7	28.9	0.81	–0.5	1.8	2.2				
Average	1.5"			0.81	1.7 (+3.3,–2.3)	1.2	2.4 (+0.5,–0.4)				

also obtained from examining the sabot strikes on the stripper cone 5.05 from the muzzle. This data is also shown in the table. The data was taken from five different stripper cones, each bearing strikes from two or more shots. Since there are strikes from several shots on each stripper cone, the sabot quarter separations recorded from the stripper strikes could not be assigned, with any degree of certainty, to specific shots of the second series.

Because of the imprecision discussed earlier resulting from the penumbra effect, the accuracy of positions read from X-rays is not as high as with photographic records, and none of these sets include simultaneous orthogonal views, which are required to define angles fully. These readings are, therefore, not precise enough for rigorous design, but they do, however, allow some interesting conclusions to be drawn.

The first series of readings was taken from tests using the 1.0" light-gas gun, with sabots shown in figure 5(a). Because of the erosion of the launch tube as discussed earlier, sabots were made in progressively increasing diameters, so that they fit firmly into the tube 100 to 150 mm from the end face of the launch tube. This meant that, for a tube nearing the end of its life, as the sabot starts to accelerate down the gun barrel, its diameter would have to decrease by some combination of elastic and plastic deformation, and possibly wear, by as much as 0.78 mm or 3.1 percent of the original tube diameter. With the X-rays in use at the time, it was not possible to read sabot segment dimensions accurately enough to define what combination of the three processes was acting. The second series of tests was conducted using the 1.5" gun, and the sabot design shown in figure 5(b). In this case, the diameter was relieved to less than the main (uneroded) launch tube diameter except for three lands, each extending about 12 percent of the length.

It is easy to show, by considering the aerodynamic forces and moments upon the separating sabot sectors, that, during the first part of the separation process, one expects both the normalized separation, $\phi = y/D$ and the sabot opening angle, θ to be roughly proportional to

$$\varphi = \frac{\rho_g x^2}{\rho_s D^2}$$

where y is the sabot separation distance, D is the barrel diameter, x is the distance from the muzzle, ρ_g is the sabot stripping gas density and ρ_s is the sabot density. We will refer to φ as the density-distance parameter. From the data of table 1, we can calculate the φ values for all the shots from the 1" gun at the two distances from the muzzle, 1.12 and 2.034 m and likewise for the 1.5" gun for the distances of 0.81 and 5.05 m from the nozzle exit.

We have also calculated the corresponding normalized sabot separations, ϕ and the sabot opening angles in radians. Only a single average value of φ and ϕ were calculated for the data for the 1.5" gun 5.05 m from the muzzle, since, as mentioned above, one could not attribute the sabot separation data to specific shots. For the three sets of angle data, only one average value of φ and θ were calculated for each data set, due to the rather large scatter of the angle data. (Note that angle data was not available for the 1.5" gun 5.05 m from the muzzle.)

Before proceeding with the analysis of the sabot separation data, we note that there are slight differences in the forms of the sabots for the 1" and 1.5" guns, creating slight differences in the aerodynamic force and moment coefficients for these two classes of sabots. It is anticipated that these slight differences will not cause the separation dynamics of the two types of sabots to different in any significant way. Hence, we will treat the data for both guns together in the following discussion. Figure 6 shows the normalized sabot separation and sabot opening angle data plotted against the distance-density parameter. We first discuss the separation data (solid data points). The round data points are for the 1" gun and the square data points for the 1.5" gun. For each gun, the points grouped at the larger value of φ are for the larger distance from the muzzle shown in table 1. We note that all four sets of data, over a 30 to 1 parameter range, lie within ±30 percent of a line drawn with ϕ proportional to φ. This suggests (1) that the sabot separation dynamics for the data shown here can be fairly well explained by the simple aerodynamic arguments referred to above and (2) that the sabots for the 1" and 1.5" guns do, indeed, separate with very similar dynamics.

We next discuss the sabot opening angle data (open data points). The round data points are for the 1" gun and the square data point is for the 1.5" gun. For the 1" gun, the point at the larger value of φ is for the larger distance from the muzzle shown in table 1. The sabot opening angle data clearly has a much larger scatter than the sabot separation data. Hence, in figure 6, we have plotted only the average opening angle for each of the three groups of data. The averaged angle data plotted in figure 6 is reasonably consistent, over a 15 to 1 parameter range, with the simple aerodynamic model which predicts that θ should be proportional to φ. (The best fitting line with θ is proportional to φ is shown dashed in fig. 6.) The two points above the trend line are about 15 percent high, whereas the point below the line is about 50 percent low.

All of the shots with the 1" gun were successful. In the case of shot A1906, with a sabot opening angle at 1.12 m

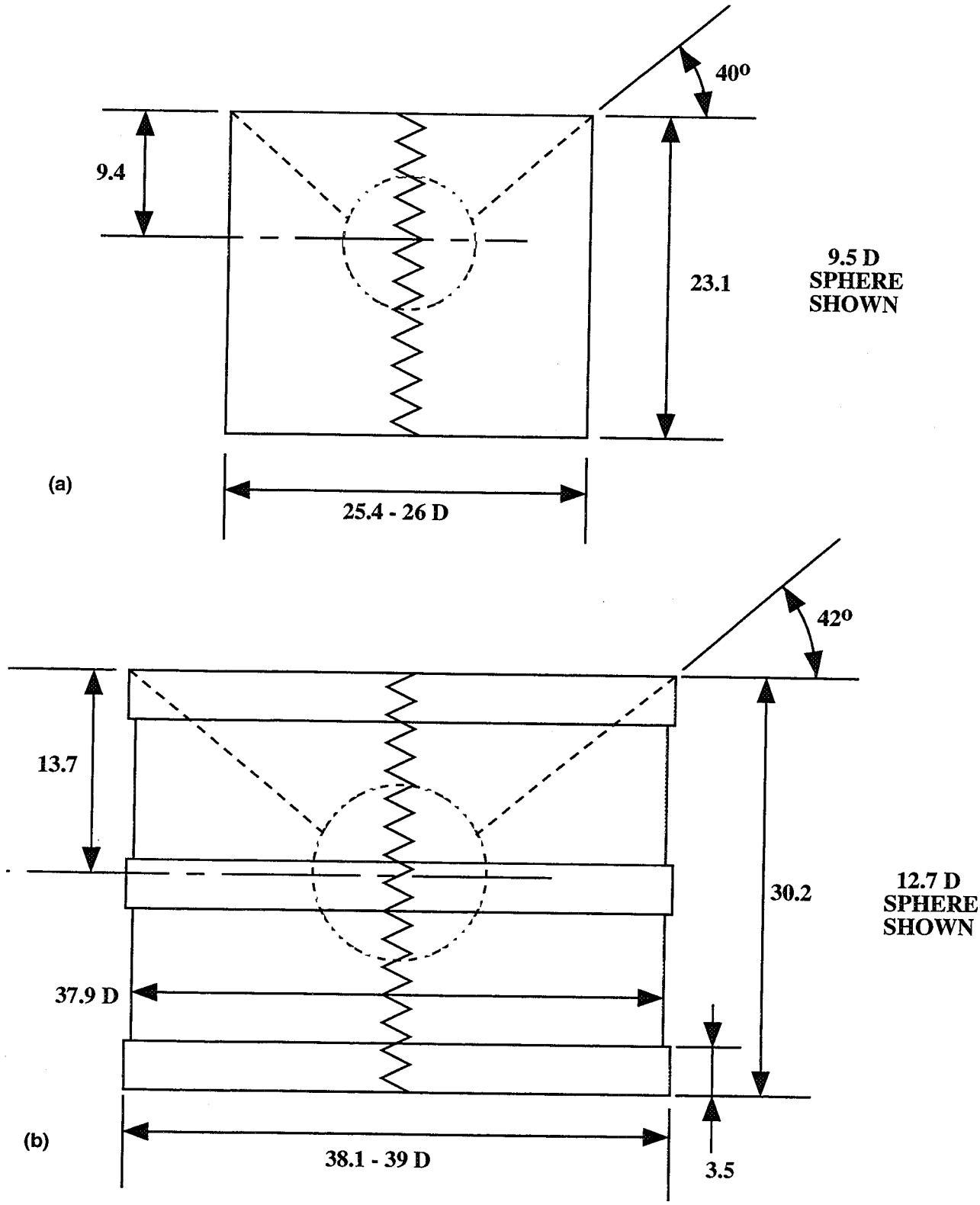

Figure 5. Sabot designs. (a) For Ames 1.0" gun with smooth outside diameter, (b) for Ames 1.5" gun with 3 lands and relieving cuts. Sabots are made in four quarters which fit together along the saw-tooth cuts.

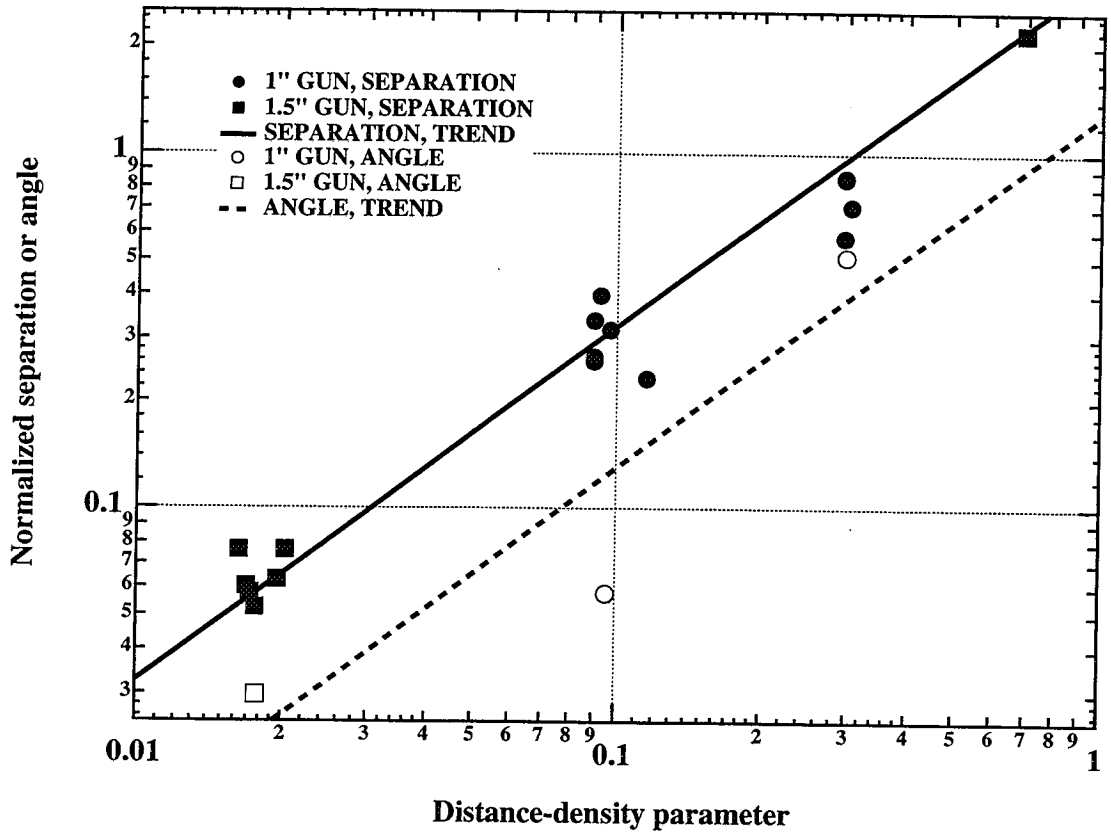

Figure 6. Normalized sabot separation or angle versus the distance-density parameter for a number of shots on the NASA Ames 1.0" and 1.5" guns.

from the muzzle of the relatively small value of 1.4 deg, the separation at 2.034 m from the muzzle was at the higher end of the scatter range. We note that three of the seven shots with the 1.5" gun had sabot opening angles 0.81 m from the muzzle which were effectively zero. (Because of the angle of the conical separation cavity, a zero angle is still expected to produce an aerodynamic separation force.) Despite these smaller sabot opening angles, the separation process was completely reliable and consistent for all shots for the 1.5" gun. There appears to be a somewhat smaller scatter in the sabot separation data for the 1.5" gun, 0.81 m from the muzzle (about 19 percent) than for the 1" gun, 1.12 m from the muzzle (about 27 percent).

The radius difference between the lands and the relieved areas on the second-series sabots were measured with some confidence, since penumbra and penetration effects were expected to be comparable in the two areas. For six shots, the radius differences before firing were 1.384 ± 0.013 mm and those after firings, measured from the X-ray photographs, were $1.524^{+0.152}_{-0.127}$ mm. The values after firing were larger by 0.025–0.28 mm. This leads to the conclusions that (1) the measuring accuracy was approximately 0.28 mm and (2) the wear during launch was very close to zero, a rather surprising observation. Furthermore, examination of figure 1 indicates that the relief areas are straight and well formed, and thus that there was no detectable plastic deformation. If this is indeed true, then the entire deflection of the sabot diameter in traversing the launch tube would appear to be elastic. This is rather remarkable, since computational fluid dynamics (CFD) calculations (refs. 6 and 7) of the maximum sabot base pressures for conditions very similar to those of shots R608-R617 yielded values of about 1600 bar, well above the quoted low strain rate compressive strengths (ref. 8) of 690–860 bar for Lexan (polycarbonate). This unexpected behavior may be similar to

the apparent ability of the polyethylene piston in the Ames 1.5" light gas gun to behave as though its high strain rate yield stress (during the gun firing cycle) is substantially higher (ref. 9) than its low strain rate value quoted in the literature.

There is a region of flight just outside the muzzle where the projectile is immersed in a flow of propellant gases escaping from the gun. This region is characterized by flows passing over the model in the reverse direction from normal flight, and by rapidly changing environment as the propellant gases expand into the atmosphere beyond the muzzle. Properties within this so-called "intermediate ballistics" region have been studied, as in reference 10, but no analysis has been done at NASA Ames to define the behavior or extent of this region. The low pressure outside the muzzle (20–50 Torr), the high propagation velocity of the hydrogen propellant, and the chemical reactivity at the hydrogen/air interface very likely make the region large and complex, when compared to the more common case of powder driven weapons firing into atmosphere. The actual intermediate ballistics environment for two-stage light gas guns is very poorly understood.

In the intermediate ballistics zone, with reversed flow over the sabot, the sabot is usually not shaped to generate gas dynamic forces tending to produce separation. It may, however, have substantial elastic energy stored as a result of the radial compression in the launch tube that is released rapidly as it emerges from the muzzle, and this momentum may provide the dominant separating action during the critical initial stage. The strain energy in a uniform cylindrical Lexan sabot with a radial stress at the compressive yield strength (assumed here to be 690 bar (ref. 8)) can readily be calculated. If all this energy is assumed to be converted into radial kinetic energy, the radial velocity of the sabot quarters, upon exiting the muzzle, can be calculated to be 42.5 m/sec. For a launch velocity of 6.6 km/sec, this translates to a sabot quarter separation, at a distance of 1.12 m from the muzzle, of 14.4 mm. Comparing this to the observed values of 6–10 mm (for the first series of table 1), it appears that this elastic energy may be capable of producing the observed sabot separations. There may be, of course, many unknown differences between this simple model and the actual situation. In particular, the actual in-barrel sabot radial stress state may be very complex and the efficiency of the conversion of the sabot strain energy into radial kinetic energy is unknown. The sabots of the second series of table 1 would have a smaller fraction of their mass affected by this radial compression, since the lands bear on the gun barrel for only about 36 percent of the total sabot length. Hence, the release of stress at the muzzle should produce less separating momentum.

There is a difficulty with the explanation that elastic energy is responsible for a significant part of the initial sabot separation process. Such an explanation would appear to predict a correlation between the progressively increasing diameter of the eroding gun barrel, hence the amount of radial compression that the sabot in subjected to when it is initially set into motion, and the extent of the sabot separation observed at the first X-ray station. Neither series of shots of table 1 shows a readily apparent correlation of this sort.

IV. Gun Barrel Erosion

A. General

An undesirable result of the high temperature of the hydrogen driver gas is the erosion of the inside bore of the gun barrel. This erosion is costly because it requires relining or replacing gun barrels after some tens of shots, and degrades performance by adding iron vapor to the otherwise low molecular weight hydrogen gas. A criterion for a peak temperature of 1200K in the steel tube wall to realize zero erosion has been reported in reference 11. The gun barrels were measured during several series of shots to attempt to characterize erosion. The depth of measurements along the tube axis was limited by the available telescoping gages, so it was not possible to determine at what depth the erosion decreased to zero. We note that approximately the first caliber of gun barrel depth is modified by a radius and a relief for the petalling diaphragm (break valve).

Table 2 gives the gun operating conditions for the gun erosion data to be discussed in this section. Data from three guns (0.5", 1.0", and 1.5") at the NASA Ames Research Center are included. For the Ames 0.5" and 1.5" guns, data from several different series of shots are included. For these same two guns, data was taken with the full pump tube volume and with the pump tube volume reduced to about 60 percent of its original value. To allow easy comparisons between the data for the different guns, all masses and volumes in table 2 have been normalized by the barrel diameter cubed (D^3).

Figure 7 shows gun erosion data, in terms of increasing barrel diameter, for one gun barrel liner for the NASA Ames 1.5" gun. The measurements were taken at four locations, 2, 2.67, 3.33, and 4 calibers deep in the gun barrel. These data were taken over the time period of all 22 shots shown in table 2 for this gun. Figure 8 shows gun erosion data for two series of shots on two different gun barrel liners, for the NASA Ames 1.0" gun. (We note here that the Ames 1.0" and 1.5" guns are nearly linearly

Table 2. Gun firing conditions for gun erosion data

Gun	Data date	No. of shots	Powder mass/D^3, gm/cm^3	Piston mass/D^3, gm/cm^3	Hydrogen, pressure, bar	Hydrogen mass/D^3, gm/cm^3	Pump tube length	Pump tube volume/D^3	Break valve rupture pr., bar	Projectile mass/D^3, gm/cm^3	Projectile velocity, km/sec
Ames 0.5"	1966,69	13	61–134	433–544	0.69–2.07	1.40–4.20	Full	24,900	344–1380	0.434–0.947	4.89–9.46
Ames 0.5"	1995	4	91.3–95.2	399–401	1.32–2.07	2.68–4.20	Full	24,900	289	0.572–0.686	6.28–7.37
Ames 0.5"	1995	12	85.4–96.2	345–354	1.70–3.39	2.11–4.21	Shorter	15,200	289	0.571–0.685	5.4–8.17
Ames 1.0"	1987–90	45	42.7–76.9	336–443	3.45–5.17	3.46–5.19	Full	12,300	345	0.702–2.935	4.4–6.7
Ames 1.5"	1994–95	19	50.8–59.6	309–388	3.1	2.97	Full	11,700	586–1170	0.529–0.592	5.5–6.8
Ames 1.5"	1995	3	51.3	309	4.71	2.97	Shorter	7,710	827	0.519–0.607	6.9–7.2

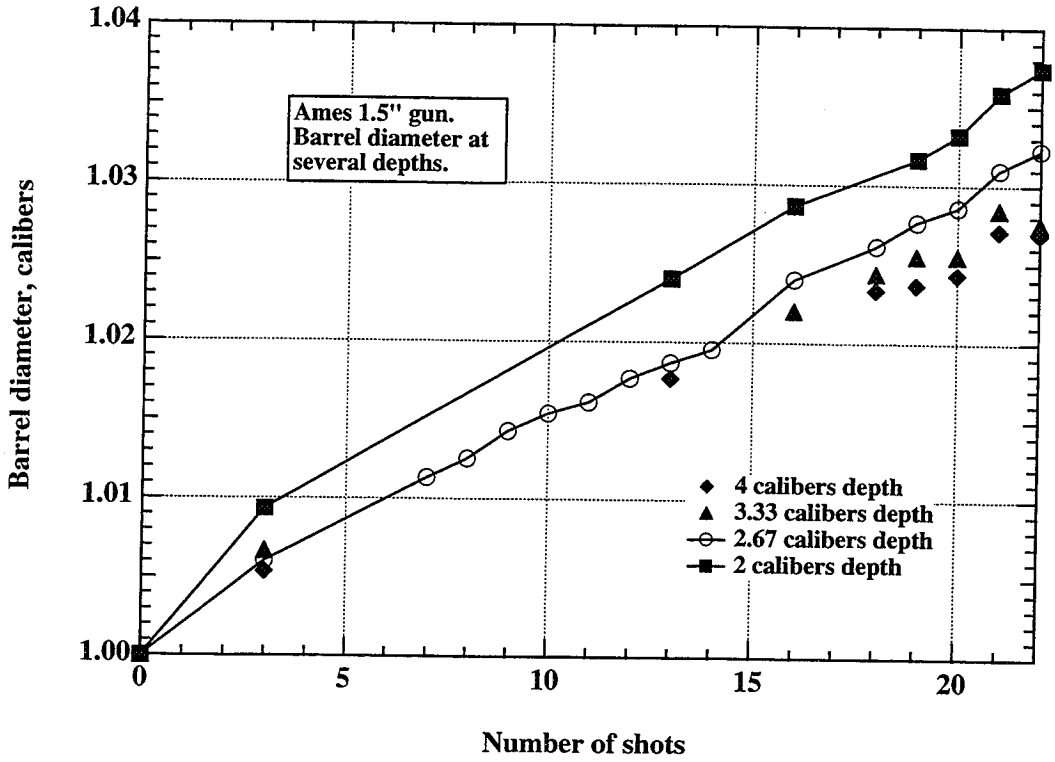

Figure 7. Barrel diameter at several depths for one series of shots on the Ames 1.5" gun.

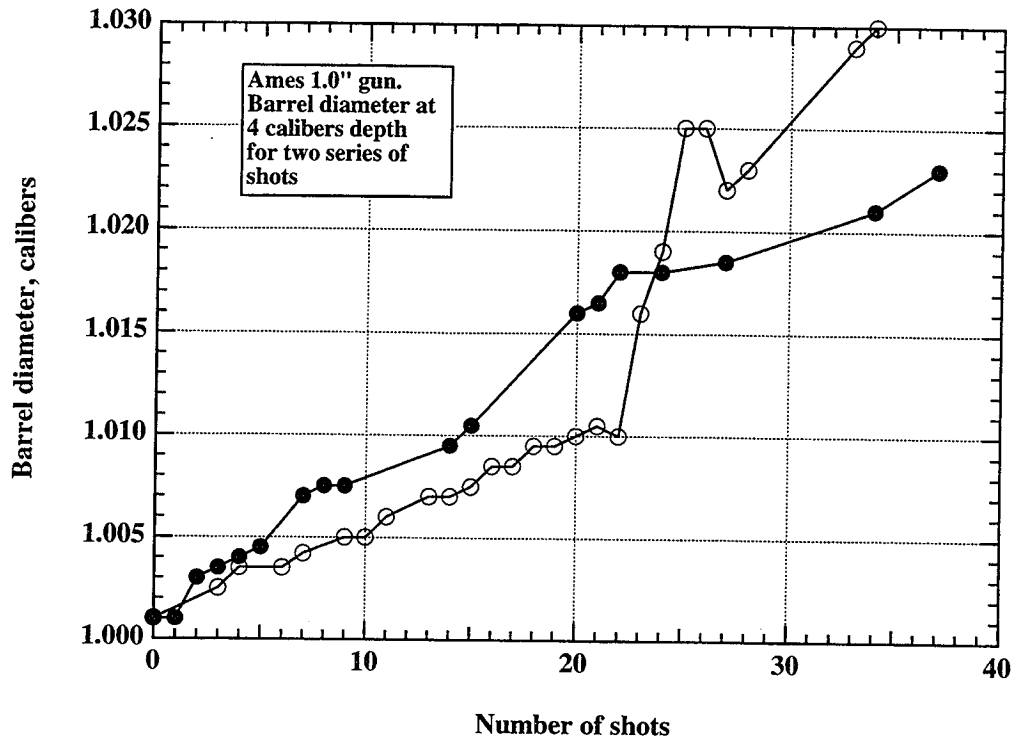

Figure 8. Barrel diameters at 4 calibers depth for two series of shots on the NASA Ames 1.0" gun.

scaled copies of each other.) The measurements were taken 4 calibers deep in the gun barrel. This data was taken for the operating conditions of the Ames 1.0" gun shown in table 2. Three different erosion rates are observed in figure 8. For the gun liner with the solid data points, a relatively constant erosion rate is apparent. For the other gun barrel liner, a lower erosion rate is noted from shots 1 to 22, followed by a sharply higher erosion rate for shots 23 to 34. The changes in the erosion rates are due to changes in the gun operating conditions–for example, increasing the powder mass or decreasing the hydrogen fill pressure will increase the gun erosion. (We will return to this issue at a later point.)

Figure 9 shows gun erosion data for two series of shots on two different gun barrel liners, for the NASA Ames 0.5" gun. (The Ames 0.5" guns is also nearly linearly scaled from the other two, larger, guns. It does have, however, about twice the normalized pump tube volume when compared to the two larger guns.) The measurements were taken 4 calibers deep in the gun barrel. This data was taken for the second and third sets of operating conditions of the Ames 0.5" gun shown in table 2. The upper curve used data form the second data set in table 2 and the first three shots of the third set of data. The barrel was then changed; the lower curve of figure 9 is from the remaining shots in the third data set of table 2. For the lower curve of figure 9, the complete barrel history is known, including the initial barrel diameter. On the other hand, for the upper curve, the barrel history before the first data point shown and the initial barrel diameter are not known. Thus, the both the abscissae and the ordinates of the upper data curve in figure 9 are somewhat arbitrary. The slope of the curve, however, can be compared with that of the lower curve. The barrel diameter of the upper curve has been normalized by the nominal barrel diameter (exactly 0.5") since the true initial barrel diameter is unknown. Initial diameters of gun barrels for the 0.5" have been measured to be as large as 0.507".

Figure 10 shows the barrel shapes measured after various numbers of shots for the Ames 1.5" and 0.5" guns. This data was taken from the same shots which yielded the data of figures 7 and 9. The erosion data for the 1.0" gun was taken at only one depth in the barrel and thus barrel shape data is not available for that gun. The data for the 1.5" gun is essentially a cross plot of the data of figure 9, with the addition of extra points measured after 22 shots. After

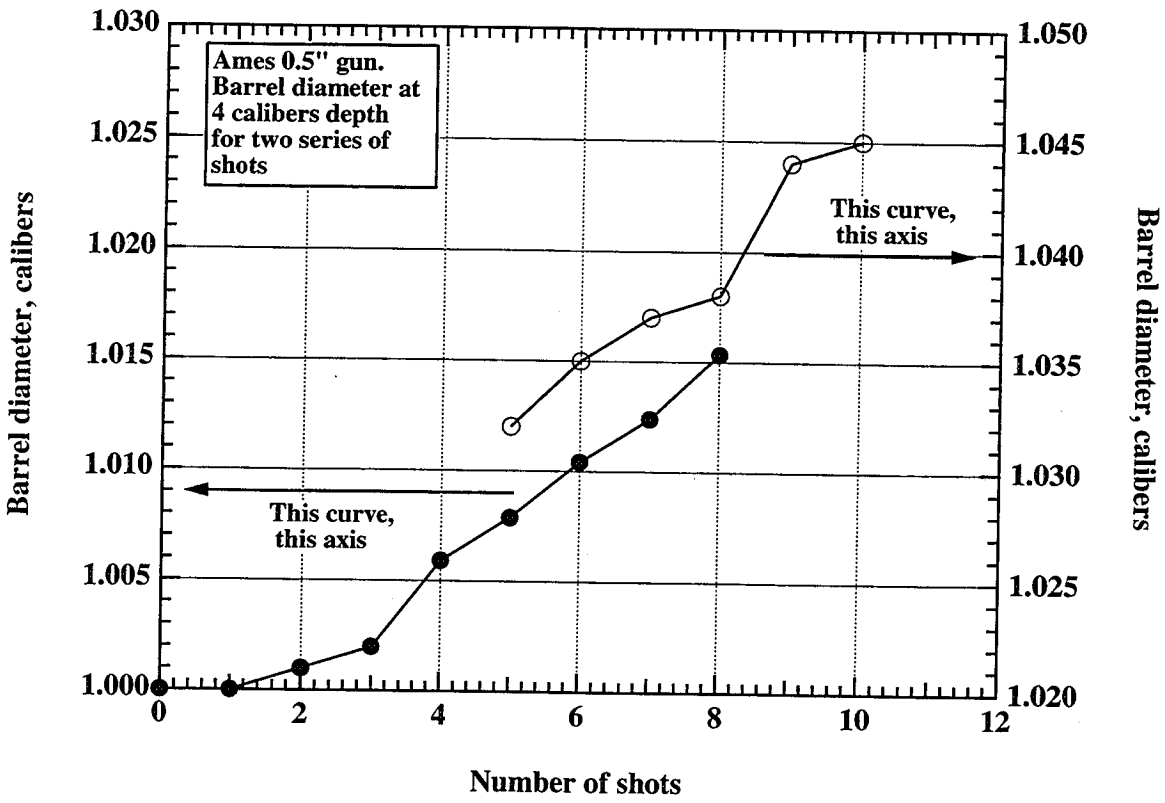

Figure 9. Barrel diameters at 4 calibers depth for two series of shots on the NASA Ames 0.5" gun. For upper curve, the absolute values of the abscissae and ordinates are not known (see text for further discussion), but the slope is correct.

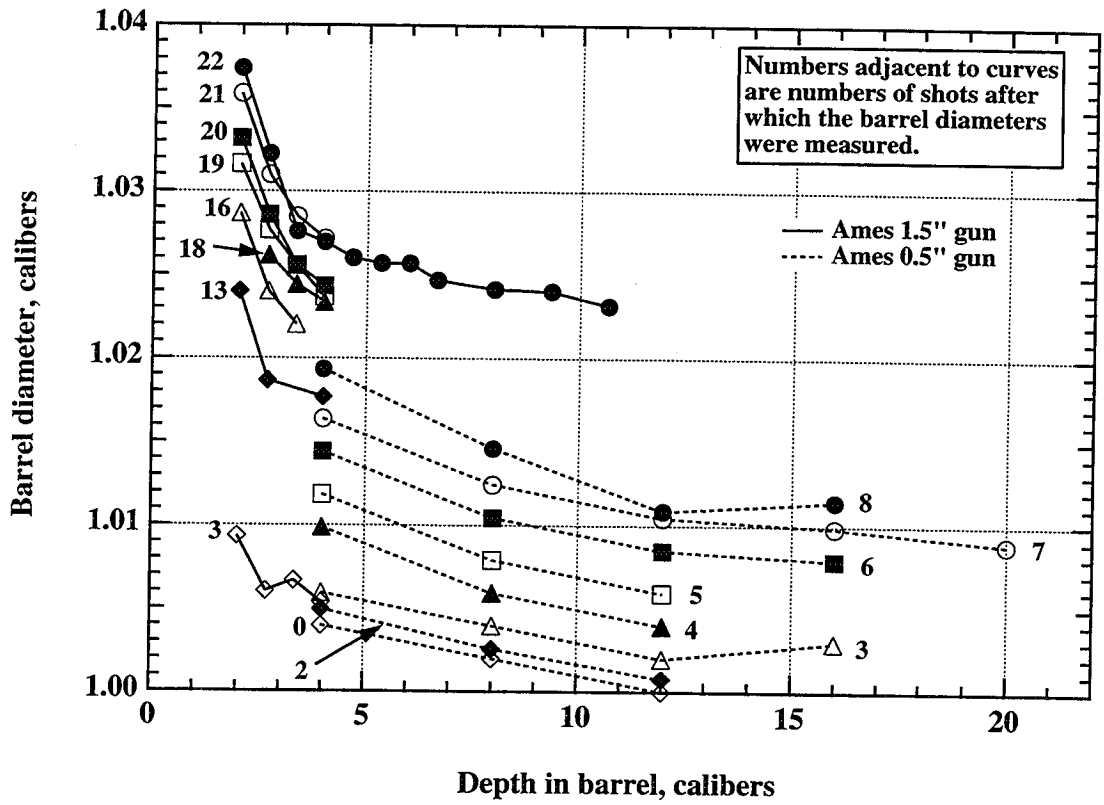

Figure 10. Barrel diameter versus depth after various numbers of shots for one series of shots on the NASA Ames 0.5" gun and one series on the Ames 1.5" gun.

22 shots, the barrel diameter was also measured at 33.3 calibers depth, and no erosion was found, i.e., the barrel diameter was measured to be exactly 1.0000 calibers at that location. This single measurement very deep in the barrel was possible because, after 22 shots, the barrel liner was removed and replaced with a new liner. The old liner was then cut up, allowing a measurement to be taken at depths normally inaccessible while the liner remains in service. The data for the 0.5" gun was from the shots in the third data set for this gun in table 2. This is for the barrel for which the complete history is known. Barrel shape data for the 0.5" gun barrel for which the complete barrel history is not known have are not given here; the location of such curves on figure 10 would be too uncertain.

The curves of figure 10, presented in normalized form, should allow one to make rough estimates for the barrel erosion to be expected in other guns, provided that the barrel erosion is known at 4 calibers depth. Obviously, the operating conditions and the gun geometries for other guns should not be too dissimilar to those of the Ames guns to allow the data of figure 10 to apply reasonably well. The Ames gun barrels are made of carbon steel. The data of figure 10 would not apply to guns whose barrels made of materials whose erosion characteristics are substantially different from those of carbon steel.

We now will attempt to correlate the gun erosion data at about 4 calibers depth with the gun operating parameters. Table 3 summarizes the quality of these data sets. The data sets listed below correspond exactly to the data sets of table 2 except that the data for the last nine shots in the third data set for the Ames 0.5" gun in table 2 is not used in the development of the present section. There are two main issues of data quality—availability of actual barrel measurements and the severity of the data grouping problem. It is obviously better to have actual barrel dimensions available. These measurements are taken with telescoping gauges which fit into the gun barrel. However, for two of the four data sets shown in table 3, only sabot diameters are available. (The original barrel measurements which lead to the selection of the steadily increasing sabot diameters for these two data sets have been lost.) For these two data sets, the barrel diameter at about 4 calibers depth (which is roughly the distance the sabot is forced into the barrel before the gun is fired) is estimated from the sabot diameters only.

Table 3. Quality of barrel erosion data at 4 calibers depth

Gun	Data date	Number of shots	Barrel diameters available	Projectile diameters available	Severity of data grouping problem	Overall data quality
Ames 0.5"	1966,69	13	No	Yes	None	Good
Ames 0.5"	1995	7	Yes	Yes	None	Excellent
Ames 1.0"	1987–90	45	No	Yes	Severe	Marginal
Ames 1.5"	1994,95	22	Yes	Yes	Minimal	Very good

The data grouping problem is as follows. For some data sets (particularly the data set for the 1.0" gun listed in table 3) barrel or sabot diameter information is not available for every shot. This means that the barrel diameter increases which are available can include the effects of two up to as many as five shots. If the shots between diameter measurements are at nearly identical gun operating conditions, the problem is minor. However, for the data for the 1.0" gun listed in table 3, there are substantial differences in powder loads and hydrogen fill pressure for some series of shots between available sabot diameter measurements. For correlating such data, these gun operating parameters must be averaged between the shots for which sabot diameter data is available. This leads to deterioration of the data. Hence, the data for the 1.0" gun is of marginal quality. The data grouping problem is of little or no consequence for the data for the 0.5" and 1.5" guns.

The data for the 0.5" gun was the most useful in developing a correlation for gun erosion. This data showed the effects of two main parameters, the normalized powder mass (M_{pn}) and the ratio of the powder mass divided by the hydrogen mass (R_{ph}), that is

$$M_{pn} = \frac{(\text{Powder mass})}{(\text{Barrel diameter})^3}$$

and

$$R_{ph} = \frac{(\text{Powder mass})}{(\text{Hydrogen mass})}$$

R_{ph} is essentially a measure of the specific enthalpy which one expects the hydrogen to be heated following the combustion of the powder, the acceleration of the piston and the compression of the hydrogen. M_{pn} is R_{ph} multiplied by the hydrogen mass and normalized by the cube of the barrel diameter. Thus M_{ph} is a measure of normalized energy content of the hydrogen gas. It can readily be shown that the erosion data for the Ames 0.5" gun correlates much better with a combination of M_{pn} and R_{ph} than with either parameter alone. The best linear combination of M_{pn} and R_{ph} was found to be ζ, where

$$\zeta = M_{pn} + 0.564 R_{ph}$$

We will refer to ζ as the powder mass parameter. The coefficient 0.564 of R_{ph} was found by plotting the gun erosion per shot versus M_{pn} and R_{ph} and estimating the average slope of the lines of constant erosion.

Figure 11 shows the correlation of the gun erosion data for the 0.5", 1.0", and 1.5" guns versus the powder mass parameter. At first, we will ignore the open data points, which are for operation with the shortened pump tubes for the 0.5" and 1.5" guns. The solid circle data points are those for the 0.5" which allowed us to determine the form of the powder mass parameter, ζ. Next, we consider the solid diamond data points, for the 1.5" gun. There are only three data points shown on figure 11 for the 1.5" gun with full length pump tube, even though there are 19 shots in this series listed in table 2. Barrel diameters were not measured for all shots, as mentioned above, and therefore, in several cases, measured barrel diameter increases include the effects of more than one shot. The data was therefore grouped into three bins. In this case, the data grouping produces little or no problem, because, when the available barrel diameter increases included the effect of more than one shot, all of the firing conditions of those shots were identical or very nearly so. That is, for the 1.5" gun, for the firing conditions between barrel diameter measurements, there was no variation of pump tube fill pressure and the powder mass variations were limited to 1 to 2 percent, except for one shot, which had a variation of 10 percent. The three data points for the 1.5" gun, all

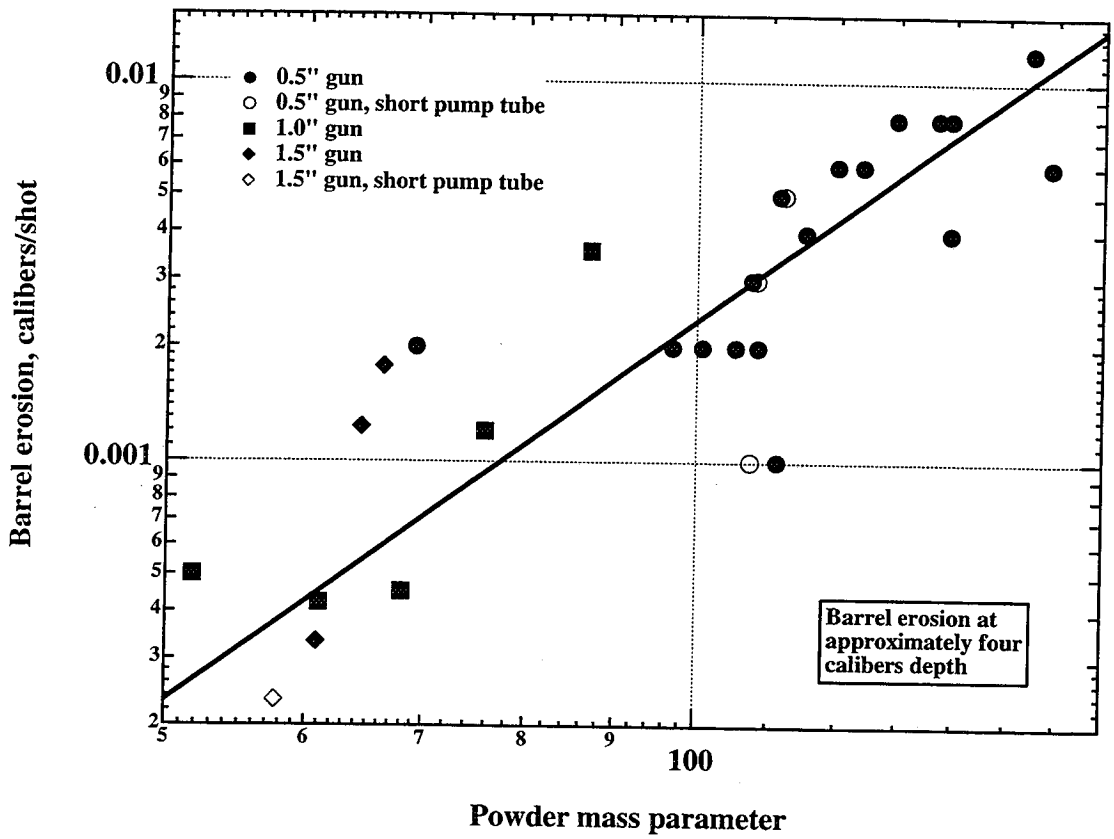

Figure 11. Barrel erosion per shot at approximately four calibers depth for the NASA Ames 0.5", 1.0", and 1.5" guns. It is plotted versus the powder mass parameter. A trend line for the data is also shown. Data with shortened pump tubes is denoted by hollow data points; for these points, the powder mass parameter has been adjusted; see text for details.

located between $\zeta = 60$ and $\zeta = 70$, are in reasonably good agreement with the extrapolated trend line from the data for the 0.5" gun.

We next turn to the data for the 1.0" gun. As mentioned early, this data had severe data grouping problems and was judged to be of marginal quality. Nevertheless, an attempt was made to plot this data on figure 11. For lack of barrel diameter measurements taken for every shot, the data for 45 shots of the 1.0" gun, of necessity, had to be grouped to provide not more than 21 data points. These were plotted on an early version of figure 11 (not shown here) and, in fact, straddled the trend line defined by the data from the 0.5" and 1.5" guns rather well, but had a very large scatter range (2 to 3 times that shown in fig. 11). To reduce the scatter, these 21 data points were then grouped in 5 bins based on the range of the values of ζ. The resulting averaged data points for the 5 bins are shown in figure 11 as the solid square data points. It is seen that the solid data points for the 1.0" guns are in reasonably good agreement with the trend line defined by the data from the 0.5" and 1.5" guns. That is, a reasonably consistent trend line can be drawn through the data for all three guns.

Note the very rapid increase in gun erosion shown in figure 11 as ζ is increased. As ζ increases by a factor of 3, the normalized gun erosion increases by a factor of 30. Figure 11, together with figure 10, showing eroded barrel shapes, should enable one to make rough estimates for gun erosion to be expected for two-stage light gas guns other than the Ames guns investigated here. Clearly, such estimates would not be expected to be reliable if the other guns differed radically from the Ames guns radically regarding (1) gun geometry/configuration, (2) normalized gun operating conditions, and (3) barrel material. Nevertheless, it is known that many two-stage light gas guns are, in fact, rather similar to those at Ames, and for such guns in service or being built or designed, figures 10 and 11 may provide useful rough estimates of erosion to be expected.

We now turn to the limited data with the shortened pump tubes. The original data yields 4 data points on figure 11. There are three open circle data points for the 0.5" gun and one open diamond data point for the 1.5" gun. On examining these data and comparing them to the corresponding data with full length pump tubes, it was clear that the reduction of the pump tube length produced a substantial reduction in gun erosion. (This effect will be discussed further in sec. IVB.) With the very limited data with shortened pump tubes available to us, the authors were not able to extract the effect of the pump tube length (or volume) in terms of a third parameter which would have corresponded to M_{pn} and R_{ph} introduced above. However, it was found that the gun erosion for shots with shortened pump tubes was very similar to that for corresponding shots with full length pump tubes at the same fill pressure. These shots with similar gun erosion do not, then, have the same hydrogen mass. In placing the data points for shots with shortened pump tubes on figure 11, an adjusted "hydrogen mass" is used. This adjusted "hydrogen mass" is not equal to the true hydrogen mass as it is for all other data points. It is based on the hydrogen fill pressure for the shortened pump tube, but the pump tube volume for the full length pump tube. This heuristic procedure brings the data points taken with shortened pump tubes into reasonable agreement with the remaining data points in figure 11. (If, on the other hand, the true values for ζ for the cases with the shortened pump tubes had been used in figure 11, these values would be 6–9 percent higher than the adjusted values and would tend, on the whole, to make the data for the shortened pump tube cases fall significantly below the trend line of fig. 11.) This discussion allows one to make very rough estimates of how shortening the pump tube might be expected to reduce gun erosion. We emphasize again that our data in this regard is limited and the authors would welcome additional gun erosion data in connection with changes in pump tube volume from other workers.

B. Changes in Gun Operating Conditions Used at Ames to Reduce Gun Erosion

We first discuss work done on the Ames 1.5" gun. Table 4 presents data on barrel erosion per shot for the Ames 1.5" gun. This data is for the same shots for which data was given in figures 7, 10, and 11. As mentioned previously, there are considerable amounts of scatter in the erosion data. Hence, in addition to the basic data, we have averaged the erosion rates at the four depths to provide the averaged data shown in the last column. This averaged data provides, perhaps, the best assessment of the effects of changing gun operating conditions on the erosion rate. The first three rows of data are grouped by powder load and yield the solid diamond data points plotted in figure 11. On increasing the powder mass parameter, ζ, from 64.42 to 66.28, the erosion is seen to increase by 72 percent. On the other hand, on decreasing ζ from 64.42 to 60.82, the erosion is seen to decrease by 30 percent. These are the same changes evident in figure 11.

After the tests of the third row of table 4, two segments of the pump tube of the gun were removed, reducing the pump tube volume by 33 percent. The hydrogen fill pressure in the pump tube was correspondingly increased to maintain the mass of hydrogen constant. Three shots were then made with the reduced pump tube length. Two of these shots were very successful; erosion data for them is reported in row 4 of table 4. It is seen that reduction of the pump tube volume by 33 percent, while maintaining the hydrogen mass, resulted in a 35 percent reduction in gun erosion, a very substantial improvement. Furthermore, this reduction in gun erosion was accompanied by an increase in muzzle velocity from 6.82 km/sec to about 7.1 km/sec. The data point for these two shots with reduced pump tube length is the open diamond point in figure 11 (based on the adjusted powder mass parameter).

On one shot with the reduced pump tube length, the hydrogen pump tube gas charge was inadvertently contaminated with 16 percent helium and 5 percent air. The data for this shot is given in the last row of table 4. It is seen that this contaminated pump tube gas leads to very greatly increased barrel erosion. (Helium is well known to be highly erosive as a pump tube gas.) The average erosion noted for this shot was 4.4 times that for the other two shots with reduced pump tube length, 2.9 times that for the shots with full pump tube length and reduced powder mass and even 2.0 times that for the shots with full pump tube length and the higher powder charge (2995 gm). In addition, the muzzle velocity for this shot was greatly reduced, from about 7.1 km/sec to about 5.5 km/sec.

We now discuss work done on the Ames 0.5" gun. In figure 12, we show the gun erosion, in calibers/shots, for the series of shots on the Ames 0.5" shown in table 3. We have added trend lines for the old data and two groupings of the new data, with the full length and the shortened pump tube. Very few changes have been made in the gun operating parameters from the 1960s data shown here up until the present optimization effort. The data from the 1960s shown in figure 12 is virtually the only good data taken previous to the 1990s for the Ames 0.5" gun with gun operating parameters anywhere near those now being used. All gun erosion data is taken at about 4 calibers depth in the barrel. The projectile mass for the seven recent shots varied between 1.17 and 1.35 gm, the average being 1.26 gm. To allow for the variation in projectile mass for the various shots, the muzzle velocities were

Table 4. Gun barrel growth per shot for Ames 1.5" gun

Powder mass, gm	Powder mass parameter		Remarks	Number of shots	Gun barrel growth, calibers per shot				
					Depth, calibers				Average for all depths
	True	Adjusted			2	2.67	3.33	4	
3082	66.28	–		3	0.00311	0.002	0.0022	0.00178	0.00227
2995	64.42	–		10 to 13	0.00149	0.00138	0.00118	0.00123	0.00132
2831	60.82	–		1 to 3	0.001	0.00122	0.00118	0.00033	0.00093
2835	60.98	57.66	Shorter pump tube	2	0.00153	0.0011	–0.00043	0.00023	0.00061
2835	60.98	57.66	Shorter pump tube + helium	1	0.00267	0.0024	0.00293	0.0028	0.0027

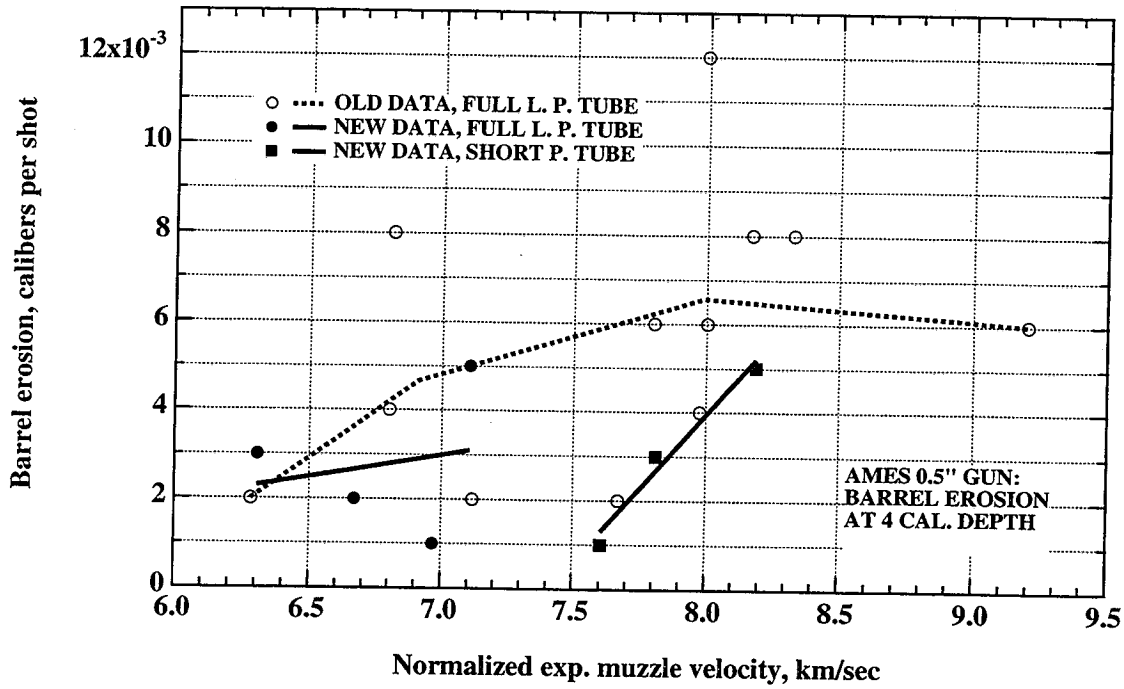

Figure 12. Barrel erosion per shot plotted versus normalized projectile velocity for several series of shots on the NASA Ames 0.5" gun. Data is shown for two series of shots with the full length pump tube and one series with the shortened pump tube. Trend lines for the three sets of data are also shown.

normalized, on a kinetic energy basis, to a projectile mass of 1.26 gm. That is, if the true muzzle velocity of a 1.17 gm projectile was 8 km/sec, its normalized muzzle velocity would be $(1.17/1.26)^{0.5} \times 8 = 7.71$ km/sec. The normalized muzzle velocity is the ordinate in figure 12. The same normalization procedure was followed for the data from the 1960s, for which the projectile mass varied from 0.89 to 1.93 gm.

The piston masses for the old data were between 888 and 1115 grams, whereas for the new data, lighter pistons with masses between 707 and 821 grams were used. For some of the low performance data from the 1960s, powder masses of 125 (for one shot) and 175 gm were used, but for most of the higher performance 1960s shots, the powder masses ranged from 200 to 275 grams. The hydrogen fill pressures for the data from the 1960s was between 0.69 and 2.07 bar. Only the last three shots of the recent data set has the benefit of the shortened pump tube. For all except one of the shots in the 1960s, the break valve pressure had the very high value of 1380 bar, whereas for the shots in the 1990s, the break valve pressures are only 289 bar. The conditions for the shots in the 1990s (even with the full length pump tube), have been selected guided by an extensive CFD optimization study which indicated that improved gun performance could be obtained at conditions considerably different from those used in the 1960s. Further details of this optimization effort are given in reference 12.

The typical large scatter of the erosion data is again evident in figure 12. A rough assessment of accuracy can be made by grouping data for similar (but not identical shots) and giving the mean and the total scatter range for the grouped data. For example, for the 1960s data between 6.8 and 7.1 km/sec, the erosion can be given as $0.0047^{+0.0033}_{-0.0027}$ calibers/shot (3 data points). For the 1960s data between 7.6 and 8.4 km/sec, the erosion can be given as $0.0067^{+0.0053}_{-0.0047}$ calibers/shot (7 data points). For all of the new data grouped together, the erosion can be given as $0.0029^{+0.0021}_{-0.0019}$ calibers/shot (7 data points). For the new data with the shortened pump tube, the erosion can be given as $0.003^{+0.002}_{-0.002}$ calibers/shot (3 data points). Although it clearly would be better to have data with better statistics, the author believes the data shown in figure 12 is strongly indicative of substantial reductions in gun erosion achieved as a result of the CFD optimization process. For example, even with the standard length pump tube, one may make an argument for about a factor of 1.5

reduction in gun erosion between the 1960s and the present, optimized gun operating conditions for normalized muzzle velocities between 6.6 and 7.2 km/sec. Comparing the new data with the shortened pump tube with the old data for normalized muzzle velocities between 7.5 and 8.4 km/sec, we see strong evidence for about a factor of 2 reduction in gun erosion achieved as a result of the CFD optimization process.

A new CFD gun code (ONEDIM) written at Ames, was used to guide certain changes in the operating conditions of the Ames 1.5" and 0.5" guns. A description of the code and code validation are presented in reference 6 and additional details of the use of the code to optimize operation of the Ames 1.5" gun are given in reference 7. The changes of the gun operating conditions from those of row 2 in table 4 to those of row 3 were guided by code predictions. These changes included the reduction in powder mass shown in table 4 as well as a reduction in piston mass from 21.42 kg to 17.06 kg. These changes produced the 30 percent reduction in gun erosion mentioned earlier, as well as a modest increase in muzzle velocity, from 6.72 to 6.82 km/sec. A second set of changes of gun operating conditions guided by the code was also instituted. These changes were those between the conditions shown in rows 3 and 4 of table 4. As mentioned previously, this involved reducing the pump tube volume by 33 percent, while maintaining the same hydrogen mass. Along with the pump tube volume reduction, the break valve (diaphragm) rupture pressure was reduced from about 1200 bar to about 800 bar. These changes resulted in a further 30 percent reduction in pump tube erosion, mentioned above, and a significant further increase in muzzle velocity, from 6.82 to 7.22 km/sec, for one of the good shots. For the other good shot with the reduced pump tube length, a considerably heavier projectile was used, 33.8 gm versus 29.5 gm. Even with the heavier projectile, the reduced pump tube length produced a velocity increase, from 6.82 to 7.06 km/sec.

The CFD optimizations process for operation of the Ames 0.5" gun is described in detail in reference 12. In that reference, it was noted that shortening of the pump tube resulted in an increase in maximum muzzle velocity (for projectiles weighing 1.17–1.35 gms) from 7.35 to 8.2 km/sec. The latter velocity considerably exceeds the previous all-time maximum velocity for this gun with saboted spheres—7.4 km/sec. These increases in muzzle velocity were obtained with reductions of barrel erosion of 30–50 percent, as noted above.

The CFD code was judged to be very valuable in selecting the best operating conditions for the Ames 0.5" and 1.5" guns.

V. Summary and Conclusions

We have described a number of recent findings in work done at the Hypervelocity Free Flight (HFF) facility (ballistic range complex) at NASA's Ames Research Center. Behavior of sabots during separation and projectile-target impact phenomena have long been observed by means of short-duration flash X-rays: most of the photographs taken to date have used "hard" X-rays. The hard X-ray techniques frequently result in rather poor definition of the object in question. Newer X-ray systems also allow operation in the lower-energy ("soft") X-ray range. Photographs taken with hard and soft X-rays have been presented and significantly improved definition was observed using the soft X-rays for certain objects. Soft X-rays were shown to produce excellent pictures of sabot separations and of debris clouds produced upon impact. Hard X-rays were shown to remain useful for viewing events deep within blocks of material.

The dynamics of sabot-separation for the Ames 1.0" and 1.5" guns has been investigated in some depth. X-ray photographs were studied at two different distances from the muzzle for the 1.0" gun. Only one set of X-ray data was available for the 1.5" gun, but this was supplemented by data obtained from the sabot strikes on the sabot stripper cone considerably farther from the muzzle. Two different sabot designs were studied. The first had a constant outside diameter which rode on the barrel wall. The second design had three lands, totaling 36 percent of the sabot length, bearing on the tube bore; the remainder of the sabot diameter was undercut, to run free of the barrel bore. The separation process for the sabots for the 1.0" and 1.5" guns was found to be reasonably consistent with the conventional aerodynamic theory. The sabots for the two guns were found to have very similar separation dynamics.

The sabot is significantly compressed radially in the gun barrel. There is thus a certain amount of elastic energy stored in the sabot while it traverses the barrel. Upon muzzle exit, this energy is available to initiate lateral sabot separation. The sabots with three lands would have much less elastic energy available than those which bear on the barrel wall for the entire sabot length. The sabots with three lands also show no evidence of wear or elastic deformation within the barrel. This observation was surprising, since the base pressures expected on the sabot substantially exceed the published low strain rate yield stress for the sabot material. This anomalous behavior of the sabot material may be related with similar anomalous behavior of the pump tube pistons observed elsewhere (ref. 9).

A detailed study of gun erosion data for the NASA Ames 0.5", 1.0", and 1.5" guns has been presented. The data shows a very strong correlation with the powder mass parameter, which is a linear combination of the powder mass divided by hydrogen mass and the powder mass divided by the barrel diameter cubed. The data sets for the three guns were found to agree fairly well with each other. The barrel erosion is shown to increase very rapidly as the powder mass parameter increases. As the powder mass parameter increases by a factor of 3, the gun erosion increases by a factor of 30. Representative shapes of eroded gun barrels have been presented. Guided by a new NASA Ames CFD code (ONEDIM), two sets of changes of gun operating conditions have been implemented for the Ames 0.5" and 1.5" guns. The first involved a decrease in the piston mass, powder load and, at times, the hydrogen fill pressure. The second involved reducing the pump tube volume by 30–40 percent, while maintaining the mass of hydrogen and reducing the break valve (diaphragm) rupture pressure. The two changes taken together produced increases in muzzle velocity from 0.5–0.8 km/sec, together with decreases in gun erosion by 30–50 percent. The code was thus judged to be very helpful in the selection of operating conditions of the Ames 0.5" and 1.5" guns. On one shot with the 1.5" gun, the hydrogen pump tube gas charge was inadvertently contaminated with 16 percent helium and 5 percent air. The contaminated pump tube gas lead to very greatly increased barrel erosion. The average erosion for this shot was about four times greater than the corresponding reference shots and the muzzle velocity was greatly reduced, from about 7.1 to about 5.5 km/sec.

References

1. Canning, T. N.; Seiff, A.; and James, C. S.: Ballistic Range Technology. AGARDograph, vol. 138, Aug. 1970.
2. Canning, T. N.; Seiff, A.; and James, C. S.: Ballistic Range Technology. AGARDograph, vol. 138, Aug. 1970, p. 241.
3. Canning, T. N.; Seiff, A.; and James, C. S.: Ballistic Range Technology. AGARDograph, vol. 138, Aug. 1970, pp. 99–153.
4. Canning, T. N.; Seiff, A.; and James, C. S.: Ballistic Range Technology. AGARDograph, vol. 138, Aug. 1970, pp. 9–95.
5. Miller, R. J.: Diverse Studies in the Reactivated NASA/Ames Radiation Facility: from Shock Layer Spectroscopy to Thermal Protection System Impact. Presented at the 45th Meeting of the Aeroballistic Range Association, Huntsville, Ala., Oct. 10–14, 1994.
6. Bogdanoff, D. W.; and Miller, R. J.: New Higher-Order Godunov Code for Modelling Performance of Two-Stage Light Gas Guns. NASA TM-110363, secs. 5.1, 5.6, Sept. 1995.
7. Bogdanoff, D. W.; and Miller, R. J.: Optimization Study of the Ames 1.5" Light Gas Gun. AIAA Paper 96-0099. Presented at the 34th Aerospace Sciences Meeting, Reno, Nev., Jan. 15–18, 1996.
8. 1984 Materials Selector, special issue of Materials Engineering, Dec. 1983, pp. 3–18.
9. Bogdanoff, D. W.; and Miller, R. J.: New Higher-Order Godunov Code for Modelling Performance of Two-Stage Light Gas Guns. NASA TM-110363, sec. 5.7, Sept. 1995.
10. Oswatitsch, K.: Zwischenballistik. report DVL-358, Deutsche Versuchsantalt fur Luft- und Raumfahrt, Dec. 1964.
11. DeWitt, J. R.: Configuration Development of the New AEDC 3.3 Inch Launcher. Presented at the 45th Meeting of the Aeroballistics Range Association, Huntsville, Ala., Oct. 10–14, 1994.
12. Bogdanoff, D. W.: Optimization Study of the Ames 0.5" Light Gas Gun. To be published as a NASA TM and submitted to the 1996 Hypervelocity Impact Symposium, Freiburg, Germany, Oct. 7–10, 1996.

REPORT DOCUMENTATION PAGE

Form Approved
OMB No. 0704-0188

1. AGENCY USE ONLY *(Leave blank)*	2. REPORT DATE	3. REPORT TYPE AND DATES COVERED
	March 1996	Technical Memorandum

4. TITLE AND SUBTITLE
Recent Developments in Gun Operating Techniques at the NASA Ames Ballistic Ranges

5. FUNDING NUMBERS
478-85-20

6. AUTHOR(S)
D. W. Bogdanoff* and R. J. Miller

7. PERFORMING ORGANIZATION NAME(S) AND ADDRESS(ES)
Ames Research Center
Moffett Field, CA 94035-1000

8. PERFORMING ORGANIZATION REPORT NUMBER
A-961332

9. SPONSORING/MONITORING AGENCY NAME(S) AND ADDRESS(ES)
National Aeronautics and Space Administration
Washington, DC 20546-0001

10. SPONSORING/MONITORING AGENCY REPORT NUMBER
NASA TM-110387

11. SUPPLEMENTARY NOTES
Point of Contact: D. W. Bogdanoff, Ames Research Center, MS 230-2, Moffett Field, CA 94035-1000
(415) 604-6138
*Thermosciences Institute, Ames Research Center

12a. DISTRIBUTION/AVAILABILITY STATEMENT
Unclassified-Unlimited
Subject Category – 12
Available from the NASA Center for AeroSpace Information,
800 Elkridge Landing Road, Linthicum Heights, MD 21090; (301) 621-0390

12b. DISTRIBUTION CODE

13. ABSTRACT *(Maximum 200 words)*

This paper describes recent developments in gun operating techniques at the Ames ballistic range complex. This range complex has been in operation since the early 1960s. Behavior of sabots during separation and projectile-target impact phenomena have long been observed by means of short-duration flash X-rays: new versions allow operation in the lower-energy ("soft") X-ray range and have been found to be more effective than the earlier designs. The dynamics of sabot separation is investigated in some depth from X-ray photographs of sabots launched in the Ames 1.0" and 1.5" guns; the sabot separation dynamics appears to be in reasonably good agreement with standard aerodynamic theory. Certain sabot packages appear to suffer no erosion or plastic deformation on traversing the gun barrel, contrary to what would be expected. Gun erosion data from the Ames 0.5", 1.0", and 1.5" guns is examined in detail and can be correlated with a particular non-dimensionalized powder mass parameter. The gun erosion increases very rapidly as this parameter is increased. Representative shapes of eroded gun barrels are given. Guided by a computational fluid dynamics (CFD) code, the operating conditions of the Ames 0.5" and 1.5" guns were modified. These changes involved (1) reduction in the piston mass, powder mass and hydrogen fill pressure and (2) reduction in pump tube volume, while maintaining hydrogen mass. These changes resulted in muzzle velocity increases of 0.5–0.8 km/sec, achieved simultaneously with 30–50 percent reductions in gun erosion.

14. SUBJECT TERMS
Ballistic ranges, Gun erosion studies, Sabot separation

15. NUMBER OF PAGES
24

16. PRICE CODE
A03

17. SECURITY CLASSIFICATION OF REPORT	18. SECURITY CLASSIFICATION OF THIS PAGE	19. SECURITY CLASSIFICATION OF ABSTRACT	20. LIMITATION OF ABSTRACT
Unclassified	Unclassified		